FIFTH INTERNATIONAL CONGRESS ON SOUND AND VIBRATION
DECEMBER 15-18, 1997
ADELAIDE, SOUTH AUSTRALIA

FINITE-ELEMENT METHOD ANALYSIS OF THE NORMAL AND RECONSTRUCTED MIDDLE EAR

*Takuji Koike, Hiroshi Wada and *Toshimitsu Kobayashi*

Department of Mechanical Engineering, Tohoku University, Sendai, Japan
*Department of Otolaryngology, Nagasaki University School of Medicine, Nagasaki, Japan

Many middle ear prostheses are available for reconstruction of a missing or damaged ossicle. However, there are few studies, which investigate the acoustic properties of these prostheses, and the information that could lead to the design and development of better ossicular replacement prostheses is absent from the report.

Clinical trials comparing many prostheses would be the best method of analysis, but these are difficult to perform and are contaminated by a large number of variables that are hard to control. Therefore, some experiments with ossicular substitution in animals and human temporal bones have been performed. However, animal studies are not very good for acoustic studies because of the anatomic differences, and the specimen is difficult to handle. In this study, three-dimensional finite-element models of a human intact middle ear and reconstructed middle ears using many types of incus replacement prosthesis are established. Then, an attempt is made to clarify the optimum method for reconstructing the middle ear.

INTRODUCTION

Application of Finite Element Method (FEM) enables complicated irregular geometries of biological structures to be modeled easily, and also FEM application enables their dynamic behavior to be understood in detail without experiments (Koike et al., 1997). A few investigations of FEM application to the analysis of the reconstructed middle ear have already been reported (Williams et al., 1995; Ladak and Funnell, 1996). However, the sound transmission properties of the prostheses have not been shown clearly. In this study, three-dimensional FEM models of a human intact and reconstructed middle ear using incus replacement prosthesis (IRP) are established, and the dynamic behavior and transmission factor of them are analyzed.

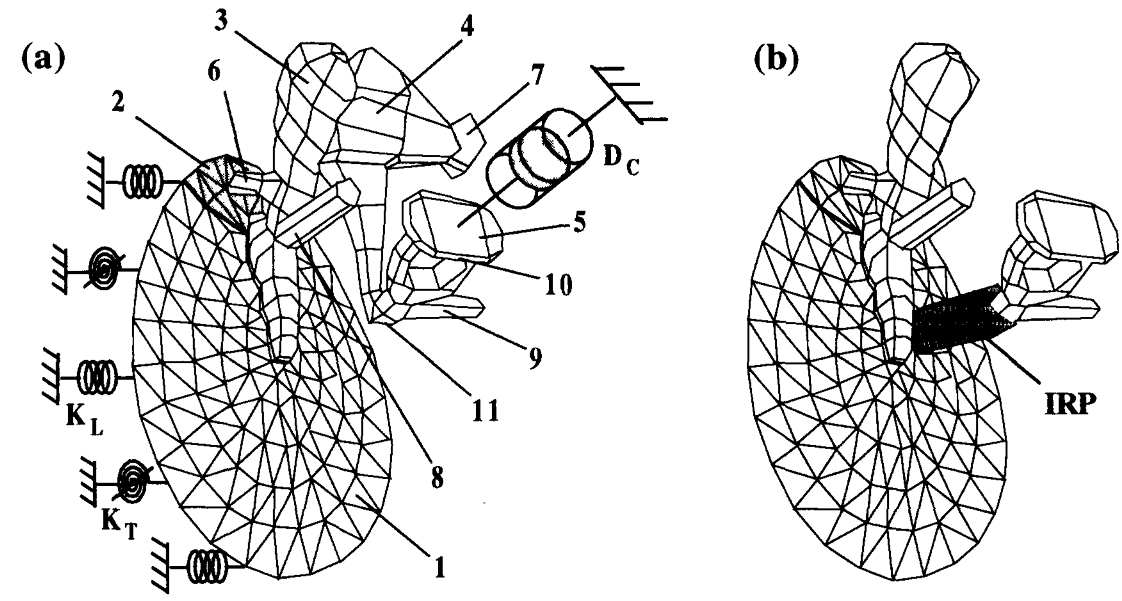

Fig. 1. FEM model of a human right middle ear. (a) Intact middle ear. Boundary condition at the tympanic ring consists of linear (K_L) and torsional (K_T) springs, and a loading of the cochlea on the stapes footplate is expressed by a damping (Dc). 1, TM (pars tensa); 2, TM (pars flaccida); 3, malleus; 4, incus; 5, stapes; 6, anterior malleal ligament; 7, posterior incudal ligament; 8, tensor tympani tendon; 9, stapedial tendon; 10, annular ligament; 11, incudostapedial joint. (b) Reconstructed middle ear. The incus is replaced by an incus replacement prosthesis (IRP) between the stapes head and near the center of the TM.

FEM MODEL

Figure 1 (a) shows the FEM model of a human right intact middle ear. The geometry of this model is based on the dimensions obtained from the study of Kirikae (1960). Two handled and thirty two flat triangular plate elements are applied to the tympanic membrane (TM). In this model, both pars tensa and pars flaccida are considered, and the Young's modulus of the pars flaccida are taken to be 1/3 of that of the pars tensa. The boundary condition at the tympanic ring consists of linear (K_L) and torsional (K_T) springs.

Eighty two hexahedral elements are applied to the model of the ossicles. The function of the anterior malleal ligament, posterior incudal ligament, tensor tympani tendon, stapedial annular ligament and stapedial tendon are taken into account. It is said that the malleus and incus vibrate as a solid body, and the incudo-stapedial joint (I-S joint) is movable. Therefore, in this model, the malleus and incus are connected rigidly, and movable I-S joint are considered by taking the Young's modulus of the I-S joint element to be smaller than that of the ossicles.

An experimental study of cochlea impedance of cat (Møller, 1965) showed that the resistive component in the normal ear was derived mainly from the cochlea. Linch et al. (1982) also reported that the input impedance took constant value of 2 MΩ (cgs), and its phase is almost zero at the frequencies from 0.5 kHz to 8.0 kHz. This result suggests that the cochlear impedance consists of a damping component.

TABLE I. Mechanical properties applied to the FEM model of the intact middle ear.

	Younng's modulus	Damping parameters	
Tympanic membrane			
pars tensa	3.34×10^{7} N / m^2	$\alpha = 260$ s^{-1}	$\beta = 3.7 \times 10^{-5}$ s
pars flaccida	1.11×10^{7} N / m^2	$\alpha = 260$ s^{-1}	$\beta = 3.7 \times 10^{-5}$ s
Anterior malleal lig.	2.1×10^{7} N / m^2	$\alpha = 0.0$ s^{-1}	$\beta = 1.86 \times 10^{-5}$ s
Posterior incudal lig.	6.5×10^{5} N / m^2	$\alpha = 0.0$ s^{-1}	$\beta = 1.86 \times 10^{-5}$ s
Tensor tympani tendon	2.6×10^{6} N / m^2	$\alpha = 0.0$ s^{-1}	$\beta = 3.72 \times 10^{-4}$ s
Stapedial annular lig.	6.5×10^{4} N / m^2	$\alpha = 0.0$ s^{-1}	$\beta = 3.72 \times 10^{-4}$ s
Stapedial tendon	5.2×10^{5} N / m^2	$\alpha = 0.0$ s^{-1}	$\beta = 3.72 \times 10^{-4}$ s
Incudostapedial joint	6.0×10^{5} N / m^2	$\alpha = 0.0$ s^{-1}	$\beta = 5.0 \times 10^{-4}$ s
Ossicles	1.2×10^{10} N / m^2	$\alpha = 0.0$ s^{-1}	$\beta = 3.72 \times 10^{-4}$ s
Cochlea		Dc = 0.624 Ns / m	

Aritomo et al. (1987) measured the cochlear impedance of the human temporal borne, and certificated that it is damping-controlled at the frequencies from 0.6 kHz to 2.2 kHz. Moreover, Zwislocki (1965) reported the human cochlear impedance is damping-controlled, and its value is about 0.35 MΩ (cgs). Therefore, in this study, the loading of the cochlea on the stapes footplate is expressed by the damping D_C.

Figure 1 (b) shows a reconstructed middle ear. The incus is replaced by an IRP. In this model, the IRP is attached to the stapes head and the TM near the center. The cross-sectional area of the IRP is 1 mm^2.

MECHANICAL PROPERTIES

The Young's modulus and the density of the tympanic membrane are determined based on the values obtained from the study of Wada et al. (1990). The Poason's ratio of the TM is 0.3. The density of each ossicles is determined based on the values which are obtained from Kirikae's work (1960). The Young's modulus of the ossicles is assumed to be uniform and was taken to be 1.2×10^{10} N/m^2 (Evans,1973).

The stiffness of the tympanic ring and the Young's moduli of the ligaments and tendons are unknown. In this study, the mechanical properties of the each part of them are determined through a comparison between the numerical results obtained from the FEM analysis and the measurement results of the manipulated temporal bone, which are obtained by the sweep frequency impedance meter (SFI) developed by our group. The damping is assumed to be in the form

$$C = \alpha M + \beta K \tag{1}$$

where C, M and K are the system damping, mass and stiffness matrices, respectively, and α and β are the damping parameters.

The mechanical properties applied to the FEM model of the intact middle ear are depicted in Table I.

MIDDLE EAR TRANSMISSION FACTOR

Middle ear transmission factor TF (= P_C / P_T) is defined as the ratio of the intracochlear pressure in the scala vestibule close to the stapes P_C to the stimulus pressure in front of the tympanic membrane P_T (Fig.2). The value of P_C is given by

$$P_C \text{ (dB SPL)} = 20 \times \log\left(\frac{2\pi f V_S Z_C}{P_{REF}}\right) \tag{2}$$

where f is the frequency, V_S is the volume displacement of the stapes footplate, $Z_C = D_C/S^2$ is the input impedance of the cochlea, S is the cross sectional area of the stapes footplate and $P_{REF} = 2 \times 10^{-5}$ Pa is the reference pressure.

NUMERICAL RESULTS

Effect of Materials

The effect of materials used for the IRP on the transmission factor is analyzed. Figure 3 shows numerically obtained TFs of intact and reconstructed middle ears using the IRPs made of four different materials, i.e., tragal cartilage, conchal cartilage, incus and hydroxyapatite. The mechanical properties of these materials are shown in Table II. The TF of the intact ear has two dull peaks at 0.7 kHz and 1.6 kHz. The TFs of IRPs made of incus and hydroxyapatite are almost the same, and show high values at high frequency regions. These are similar to the TF of the intact ear. However, the IRP made of tragal cartilage gives a sharp peak in the frequency region around 1.0 kHz, and gives a low TF at a low and high frequency region in comparison with the intact ear.

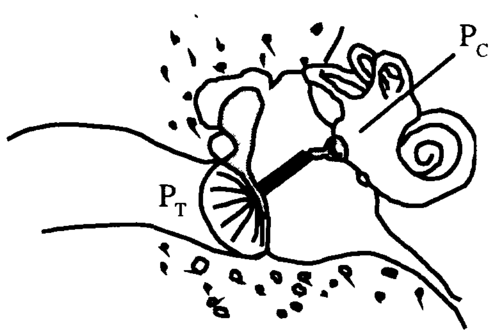

Fig. 2. Definition of transmission factor (TF). Middle ear transmission factor TF is defined by $TF = P_C/P_T$, where P_C is the intracochlear pressure and P_T is the stimulus pressure.

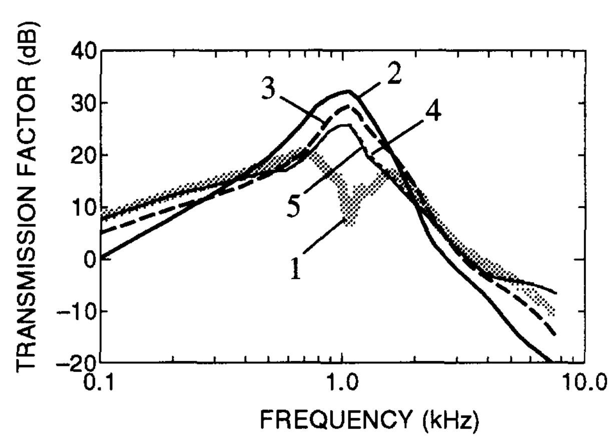

Fig. 3. Transmission factors of four different materials used for the IRP. The incus is replaced by the IRP between the head of the stapes and near the center of the tympanic membrane as shown in Fig. 1 (b). 1, Intact ear; 2, tragal cartilage; 3, conchal cartilage; 4, incus; 5, hydroxyapatite.

TABLE II. Mechanical properties of the materials used for the prostheses.

	Density	Younng's modulus	Damping parameters	
Tragal cartilage	1.1 g/cm^3	4.0×10^6 N/m^2	$\alpha = 0.0\ s^{-1}$	$\beta = 3.72\times10^{-4}$ s
Conchal cartilage	1.1 g/cm^3	1.7×10^7 N/m^2	$\alpha = 0.0\ s^{-1}$	$\beta = 3.72\times10^{-4}$ s
Incus	2.2 g/cm^3	3.7×10^8 N/m^2	$\alpha = 0.0\ s^{-1}$	$\beta = 3.72\times10^{-4}$ s
Hydroxyapatite	3.1 g/cm^3	1.55×10^{11} N/m^2	$\alpha = 0.0\ s^{-1}$	$\beta = 3.72\times10^{-4}$ s

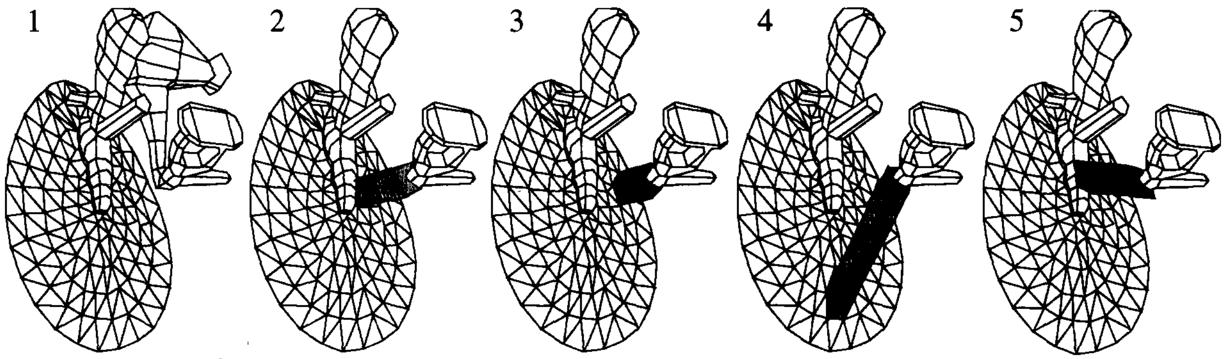

Fig. 4. Intact and four different reconstructed middle ear models. 1, Intact ear; 2, near the center point of the TM; 3, posterior point of TM; 4, inferior point of the TM; 5, the midpoint of the malleus manubrium.

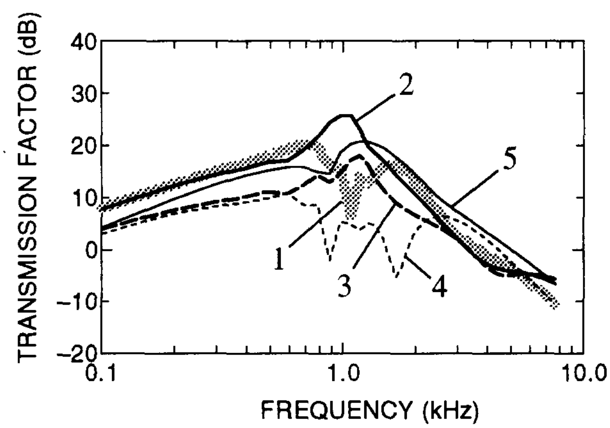

Fig. 5. Effect of the contact point on the transmission factor. The IRP is made of hydroxyapatite. Transmission factors are obtained from the models in Fig. 4. 1, Intact ear; 2, near the center point of the TM; 3, posterior point of TM; 4, inferior point of the TM; 5, the midpoint of the malleus manubrium.

This difference is closely related to the stiffness of the IRPs. When tragal cartilage, whose Young's modulus is relatively small, is used for the IRP, it vibrates with a bending motion. In contrast, when hydroxyapatite, whose Young's modulus is relatively high, is used for the IRP, it vibrates with a piston-like movement. This is one reason why the IRP made of tragal cartilage shows a low TF.

Effect of Contact Point

Next, the effect of the contact point of the IRP on the TF is analyzed. Intact and four different reconstructed middle ear models are shown in Fig. 4. The contact points of the IRP are near the center, posterior and inferior point of the TM and the midpoint of the malleus manubrium. In these models, all the IRPs are made of hydroxyapatite. Figure 5 shows the TFs obtained from these models. The IRP

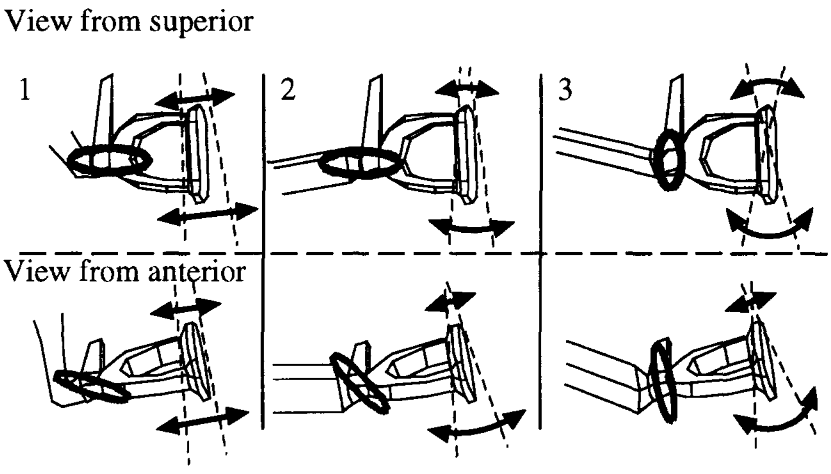

Fig. 6. Vibration mode of the stapes at the frequency of 1.0 kHz. The material and contact point are the same as those in Fig. 5. 1, Intact ear; 2, near the center point of the TM; 3, posterior point of the TM. Direction of the movement of the stapes footplate and the orbit of the stapes head are shown by allows and ellipses, respectively.

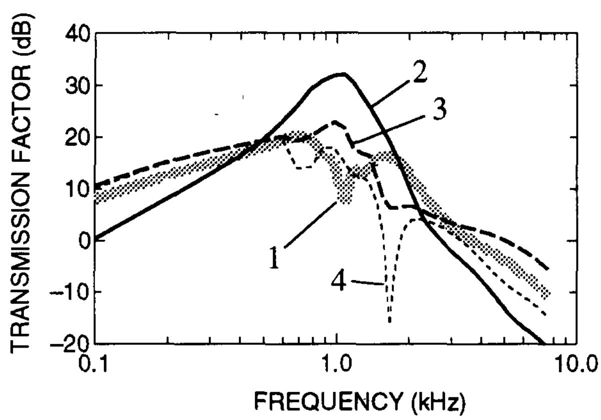

Fig. 7. Effect of the shape of IRP on the transmission factor. Transmission factors are obtained from the models in Fig. 8. 1, Intact ear; 2, the cross-sectional area of the IRP is 1.0 mm^2; 3, 16 mm^2; 4, 24 mm^2.

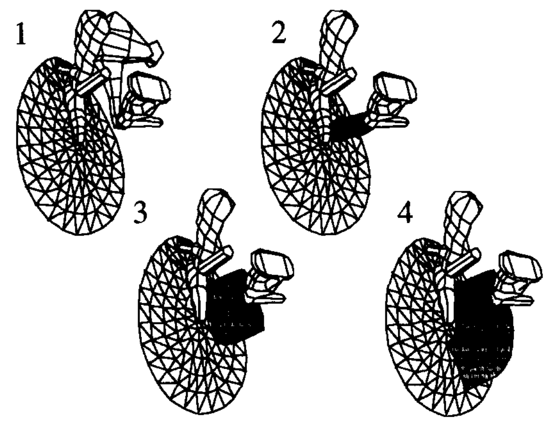

Fig. 8. Intact and reconstructed middle ear models. 1, Intact ear; 2, the cross-sectional area of the IRP is 1.0 mm^2; 3, 16 mm^2; 4, 24 mm^2.

between the head of the stapes and the malleus manubrium gives a high TF, especially for high frequencies above 1.5 kHz, whereas the contact of the IRP at the inferior portion shows the worst performance at frequencies ranging from 0.8 to 2.5 kHz.

This difference is derived from the difference in the vibration mode of the stapes. Figure 6 shows the numerically obtained vibration modes of the stapes at a frequency of 1.0 kHz. The stapes of the intact ear has a hinge-like movement as well as a piston-like movement, and the stapes head has an elliptical orbit whose long axis runs from the external auditory meatus side to the cochlear side. When the IRP is attached to the TM near the center, the vibration mode of the stapes is almost the same as that of the intact ear. In contrast, when the IRP is attached to the posterior point of the TM, the long axis of the elliptical orbit of the stapes head is perpendicular to that of the intact ear, and the stapes shows a rocking motion. This vibration mode change decreases the TF.

Effect of Shape

Figure 7 shows the TFs of intact ear and reconstructed middle ear using three different IRPs made of tragal cartilage, whose cross-sectional areas are 1 mm^2, 16 mm^2 and 24 mm^2, respectively (Fig. 8). The IRP whose cross-sectional area is 16 mm^2 shows the best performance of the three IRPs. When the cross-sectional area of the IRP is small, the vending motion occurs as mentioned above, and the TF decreases at low and high frequencies. When the cross-sectional area of the IRP is large, the TF decreases at high frequencies because of the increase in mass of the IRP.

CONCLUSIONS

Applying the finite-element program developed by our group, a three-dimensional FEM model of the reconstructed middle ear with the IRP was established, and the transfer function and the vibration patterns were analyzed. The following conclusions are drawn.

(1) High stiffness of the IRP increases the transmission factor for higher frequencies.

(2) The best contact point of the IRP is the malleus manubrium, especially for high frequencies above 1.5 kHz, whereas the contact of the IRP at the inferior portion shows the worst performance for frequencies ranging from 0.8 to 2.5 kHz.

(3) Transfer function of the IRP made of tragal cartilage varies considerably according to its cross-sectional area.

REFERENCES

Aritomo, H., and Goode, R. L. (**1987**). "Cochlear input impedance in fresh human temporal bones," 91st Meeting, American Academy of Otolaryngology, Chicago Research Forum.

Evans, F. G. (**1973**). Mechanical properties of bone, edited by C. Charles (Thomas Publisher).

Kirikae, I. (**1960**). The structure and function of the middle ear (The University of Tokyo Press, Tokyo), pp. 38-63.

Koike, T., Wada, H, and Kobayashi, T. (**1997**). "Modeling of human auditory periphery using finite-element method," Transactions of the Japan Society of Mechanical Engineers 63 - 607C, 654 - 660 (In Japanese).

Ladak, H. M., and Funnell, W. R. J. (**1996**). "Finite-element modeling of the normal and surgically repaired cat middle ear," J. acoust. Soc. Am. **100**, 933-944.

Lynch, T. J., III, Nedzelnitsky, V., and Peake, W. T. (**1982**). "Input impedance of the cochlea in cat," J. Acoust. Soc. Am. **72**, 108-130.

Møller, A. R. (**1965**). "An experimental study of the acoustic impedance of the middle ear and its transmission properties," Acta Otolaryngol (Stockh) **60**, 129-149.

Wada, H., and Kobayashi, T. (**1990**). "Dynamical behavior of middle ear: Theoretical study corresponding to measurement results obtained by a newly developed measuring apparatus," J. Acoust. Soc. Am. **87**, 237-245.

Williams, K. R., Blayney, A. W., and Lesser, T. H. J. (**1995**). "A 3-D finite element analysis of the natural frequencies of vibration of a stapes prosthesis replacement reconstruction of the middle ear," Clin. Otolaryngol. **20**, 36-44.

Zwislocki, J. J. (**1965**). "Analysis of some auditory characteristics," in Handbook of Mathematical Phychology, edited by R. O. Luce, R. R. Bush, and E. Galanter (Wiley, New York).